

Detecting passenger postures by pressure sensors under the cushion of an aircraft seat

Yufei He, Xinhe Yao, Alice Buso, Norbert Hessenberger, Yu Song, Peter Vink

Abstract

Pressure sensors could be used to determine the aircraft passenger posture or change in posture, which could indicate passengers' comfort. In this paper pressure sensors underneath the foam were used to detect the passenger posture. Additionally, an attempt was made to find the minimal number and positions of sensors that are needed to detect the posture. The pressure profiles of 12 sitting postures were collected of 33 subjects both at the top and the bottom of 3 different cushions, respectively. The experiment lasted 12 minutes for each cushion and it was tested in a static situation. Analysing the data indicated that it was possible to detect 7 types of postures with 15 sensors underneath of 3 types of cushions with an accuracy of 99.0%, which was higher than using the same amount of sensors on the top of the cushion. It was concluded that accurately detecting passenger posture using the sensors underneath the foam was possible. Further studies are needed with longer exposure time and in real flight conditions.

Introduction

In 2018 it was predicted that the number of airline passengers will double in the next 20 years (IATA,2018). However, in 2020 the airline passengers are decreasing due to the COVID-19 pandemic. In any scenario airlines try to attract passengers. Sitting comfort has been a significant factor for passengers when choosing an airline, especially for long haul flights since they spend most of their time sitting in a constrained space, sometimes even up to 15 hours (Hiemstra-van Mastrigt, Meyenborg, & Hoogenhout, 2016). The prolonged sitting can cause discomfort in the body, which could lead to serious complaints such as venous thromboembolism (VTE) (Gavish, & Brenner, 2011). Due to economic and sustainability considerations, there is not much margin for airline companies to enlarge the passenger's personal space. Therefore, analysing sitting comfort and discomfort to find the most optimal seat or seating position is important for the industry to survive in this competitive market.

In the literature sitting comfort and discomfort are often described as two subjective and independent sensations (e.g. Hiemstra-van Mastrigt, Groenesteijn, Vink, & Kuijt-Evers, 2017). These are influenced by users' mental state and anthropometric characteristics, by the product with which they interact and by the environment in which they are located: in this case the aircraft cabin (Vink, Overbeeke, & Desmet, 2004). Comfort and discomfort experiences are both reactions on the contact with the physical environment and the product. There are indications that the sitting comfort is more related to feelings of relaxation and more driven by psychosocial factors, while sitting discomfort is more related to biomechanical factors such as soreness, pain, stiffness and fatigue (Vink & Hallbeck, 2012; Zhang, Helander, & Dury, 1996). Their presence can be simultaneous and they are not linearly correlated. The sitting comfort could be reduced by increasing the sitting discomfort, however, reduction in sitting discomfort does not necessarily result in an increase of sitting comfort (Helander and Zhang, 1997).

Many studies have investigated sitting comfort and discomfort separately by applying subjective or objective measures, or the combination of them. These have been difficult to quantify due to the difference between human sensing and the many external factors that influence the five senses. Probably, those elements that lead to touch and pressure are important (Zemp, Taylor, & Lorenzetti, 2015). The human-seat interface has been investigated in many researches. There are several studies that demonstrate that over time the discomfort increases and the number of times resitting or fidgeting increases as well (e.g. Sammonds, Fray, & Mansfield, 2017; Smulders et al., 2016). These seat fidgets and movements (SFMs) can be recorded by shoulder movement, pressure distribution, peak pressure, mean pressure, centre of pressure and contact area. They might be good indicators in quantifying sitting discomfort. Intentionally taking activities in-between continuously sitting reduces discomfort. Sammonds et al. (2017) showed that long term driving comfort improved by taking breaks in which the driver walks, and Hiemstra-van mastrigt (2016) demonstrated the influence of activities and duration on comfort and discomfort

development in time of aircraft passengers. Also, the fidgeting or resitting increase in time as discussed might be an indication that the human body should move to reduce more increase in discomfort.

Ideal pressure distribution has been widely studied in car driving. For the driving seat it is suggested that 50-65% of load carried by the seat should be in the buttock area, 10-30% of the load in the upper thigh and less than 6% of the load in the lower thigh (see Figure 1 to create least discomfort (Hartung, 2006; Zenk et al., 2012). Kilincsoy (2019) conducted a similar research on an SUV with 50 subjects sitting in the rear seat and defined an ideal pressure distribution for upright position (see Figure 2), which will be used to compare the results with the aircraft seat studied in this paper since the SUV seat position is assumed to be close to the passenger position. Both models indicate that more comfort can be perceived with the limited load distributed in upper (<6%) and lower thigh (10-30%) areas (Naddeo, Califano, & Vink, 2018). In addition, it shows that the less discomfort and higher comfort are related to lower mean pressure, lower peak pressure, and higher contact area (Zemp, Talor, & Lorenzetti, 2015) and discomfort is influenced by varying the posture. This shows that recording pressure might be very useful. We could check how the pressure is distributed in the seat and it is close to the 'ideal pressure distribution' as described in the literature, but we could also see the fidgeting or resitting. Additionally, the pressure distribution is linked to the activity and we could even get an idea on what people are doing or at least an indication of what posture they take.

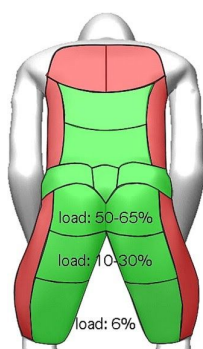


Figure 1. Ideal pressure distribution (Hartung, 2006; Zenk et al., 2012)



Figure 2. Ideal pressure distribution (Kilincsoy, 2019)

In studying pressure, the characteristics vary between different anthropometric groups. It has been found that a correlation exists between contact area and mean pressure, and BMI, hip width and other anthropometric variables (Hiemstra-van Mastrikt, Groenesteijn, Vink, & Kuijt-Evers, 2017). Also, age has its effects. For example, the subjects with greater age and height lead to higher peak pressure, and subjects with a heavier weight and higher height lead to higher mean pressure (Naddeo, Califano, & Vink, 2018). Therefore, in studying the effect of a subject on pressure the selection should not be in a certain age or length group, but having a certain variation is probably more relevant if some kind of generalisation is strived for.

In previous studies, questionnaires on comfort and discomfort ratings in questionnaires and interviews are used, which have been proven to be effective in quantifying and qualifying the sitting comfort and discomfort (Anjani, Ruiter, & Vink, 2020). The characteristics of the subjects, such as their experiences, expectations, and state of mind influence the comfort experience. In addition, perceived sitting comfort and discomfort differ from the duration of experiment, which can be divided into initial (initial 3 min), short-term (up to 30 min) and long-term (over 30 min) sitting comfort and discomfort evaluation (Mergl, 2006). These different characteristics of the subjects and the experimental setup can influence the outcome, therefore making research in this area challenging. In many cases, researchers tackled this problem by using a within subject design and having the environment and product as constant as possible.

Apart from questionnaires also recordings are made of the human-environment interaction to understand more about comfort or discomfort. Many product and user behaviour sensors are found in the literature (e.g. Le, Rose, Knapik and Marras, 2014). The real-time measurements concern often postural, biomechanics and physiological factors. For postural and activity recognition, often camera recordings, human observation, pressure sensor arrays such as pressure mats developed by Xsensor Technology Corporation, Tekscan, Inc., and Medilogic GmbH, smart fabrics and multiple single pressure sensors on the seats are described (Wegner, 2020). Specifically for the office chair, commercial smart cushions are available such as DARMA (DARMA, 2019) and SENSIMAT (SENSIMAT System, 2014). These systems monitor sitting postures and give suggestions

to improve sitting habits of the user. Given the context of an aircraft interior, it could be practical to apply sensor-based recognition methods to study aircraft passenger's sitting behavior and to see if seats are occupied..

The most used sensor to study pressure distribution and recognise sitting postures is the pressure sensor. It could be a non-intrusive manner if the sensors are embedded into the seat cushion (e.g. DARMA, 2019) or an intrusive manner using a mat placed in between the seat and the occupant (e.g. Kilincsoy, 2019). Commercial available pressure mats are widely used to evaluate and predict sitting comfort and discomfort (Romano et al., 2019; Zhao, Yu, Adamson, Ali, Li, & Li, 2020; Fasuloa, Naddeoa, & Cappetti, 2019; Naddeo, Califano, & Vink, 2018; Zenk, Franz, Bubb, & Vink, 2012). These mats are a matrix of pressure sensing points. Based on the sensor information a pressure map can be made, but also mean pressure, peak pressure, center of pressure and contact area can be retrieved using software. To reduce the influence on subject's sitting experience, thin-film type pressure sensor array has been embedded into the seat cushion for posture recognition (Liu, Guo, Yang, Hu, & Wei, 2019; Ai, Zhang, Yuan, & Huang, 2018; Bang, Kang, Choi, Mun, Tack, & Jang, 2010). Similarly, some studies have explored the use of smart textile in this application (Zhu et al., 2019; Ishac & Suzuki, 2018; Ahram & Falcão, 2018; Kim, Kim, Park, Jee, Lim, & Park, 2018; Xu, Li, Huang, Amini, & Sarrafzadeh, 2011; Mayer, Arnrich, Schumm, & Tröster, 2010). In addition to retrieve massive pressure data from human-seat interface, another method might be to distribute multiple individual pressure sensors, including Force Sensitive Resistor (FSR) sensors and load cells, on the surface of the seat or inside of the cushion in certain patterns. The goal of this paper is to define the position of each sensor making use of the least number of sensors.

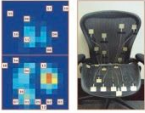



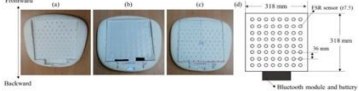
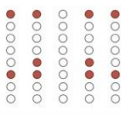
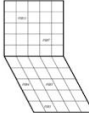


Other types of sensors are also capable of recognising sitting postures, including motion sensors, flex sensors, capacitive proximity sensors, and strain gauges, which are usually designed into wearable devices attached to the subject (Kim, Wang, Ho, Min, Kim, & Choi, 2020; Low et al., 2020; Zhang et al., 2020; Tatsuno & Maeda, 2019; Qian et al., 2018; Ma, Cho, Quan, & Lee, 2016). This is a less intrusive manner then placing a sensor mat between the seat and the occupant. There are also studies that used the fusion of the different types of sensors mentioned above, mainly the combination of FSR sensors and motion sensors (Ma, Li, Gravina, Cao, Li, & Fortino, 2017; Zemp et al., 2016). In this case, the motion sensors can be either embedded into wearable devices or placed on the seat pan or the backrest.

From an aircraft passenger's perspective, the non-intrusive manner would be preferable since it lowers the influence on sitting experience. From the airline's perspective, the power consumption, the product performance such as lifespan and maintenance, and the cost are the main criteria for technology embodiment. When balancing these considerations, the single usage of FSR sensors seems to be an optimal solution. However, it would be challenging to decide the amount of FSR sensors should be used and their placements. Therefore, their distribution pattern on the seat will be further explored.

FSR sensors distribution method

Many studies have successfully recognised sitting postures by only deploying individual pressure sensors, as summarised in Table 1. The reasons for the position of the sensors is in most of the studies not evidently-described. Some studies started with trial and error when deciding the sensor positions and the amount of these. Only a few studies conducted the research on reducing the sensor input while maintaining accuracy by firstly collecting pressure data from the pressure sensor matrix (Ma, Li, Gravina, & Fortino, 2017; Liang, Cao, & Liu, 2017; Mutlu, Krause, Forlizzi, Guestrin, & Hodgins, 2007). However, the optimised sensor positions were mostly selected in the context of placing the sensors directly on the surface of the seat and the backrest. In the study of Mutlu, Krause, Forlizzi, Guestrin, & Hodgins (2007) a low-cost, non-intrusive sensing and recognizing system was developed to detect sitting postures at an office chair. The researchers collected pressure map data from two commercial pressure mats placed on the backrest and on the seat when 52 subjects were sitting on it. It appeared that using 19 FSR sensors with their position selected based on an algorithm, could predict the human posture with an accuracy of 78%. Liang, Cao, & Liu (2017) designed a cushion to recognize sitting postures. They started with 40 cells and finally selected 10 important cells after balancing the cost and accuracy.

Table 1. Previous studies on recognizing sitting postures by using multiple individual pressure sensors and sensor matrix

Citation	No. of subjects	Data amount	No. of postures	Recognized postures	Classifier	Accuracy	No. of sensors	Sensor distribution
(Mutlu, Krause, Forlizzi, Guestrin, & Hodgins, 2007)	52	2,750 sets (5 examples*10 postures*55 subjects)	10	Left leg crossed, right leg crossed (leaning left), leaning back, leaning forward, leaning left, leaning right, left leg crossed (leaning right), seated upright, right leg crossed, slouching	Simple Logistic	78% (87% using 31 sensors)	8 on the backrest 11 on the seat pan	
(Zemp et al., 2016)	41	1,148 sets (4 examples*7 postures*41 subjects)	7	Upright, reclined, forward inclined, laterally tilted (right/left), crossed legs (left over right/right over left)	Random Forest	90.9% (81.9% using only sensors on the seat)	2 on the armrests 4 on the backrest 10 on the seat pan	
(Fragkiadakis, Dalakleidi, & Nikita, 2019)	12	1,200 sets (20 examples*5 postures*12 subjects)	5	Lean backwards, lean forward, upright position, lean left, lean right	KNN	98.33%	1 on the headrest 4 on the backrest 8 on the seat pan	
(Martins et al, 2015)	50	9,000 sets (15 examples*12 postures*50 subjects)	12	Seated upright, leaning forward, leaning back, leaning back without lumbar support, leaning left, leaning right, right leg crossed, right-leg crossed (leaning left), left leg crossed, left leg crossed (leaning right), left leg over right, right leg over left	ANN with Fuzzy Logic	80.9%	4 on the backrest 4 on the seat pan	
(Kim, Son, Kim, Jin, & Yun, 2018)	10	13,000 sets (260 examples*5 postures*10 subjects)	5	Sitting straight, lean left, lean right, sitting at the front of the chair, sitting crossed-legged on the chair	CNN	95.3%	64 on the seat pan	
(Liang, Cao, & Liu, 2017)	15	N/A	15	Sitting upright, slouching, leaning back, leaning forward (<30 degrees), leaning forward (>45 degrees), leaning left (<10 degrees), leaning left (>20 degrees), leaning right (<10 degrees), leaning right (>20 degrees), left leg crossed in ankle, left leg crossed in knee, right leg crossed in ankle, right leg crossed in knee, left leg crossed, leaning right, right leg crossed, leaning left	AdaBoost (C4.5)	98%	10 on the seat pan	
(Ma, Li, Gravina, & Fortino, 2017)	12	36,000 sets (600 examples*5 postures*12 subjects)	5	Proper sitting, lean left, lean right, lean forward, lean backward	J48	99.47%	2 on the backrest 3 on the seat pan	
(Roh, Park, Lee, Hyeon, Kim, & Lee, 2018)	9	N/A	6	Upright sitting with backrest, upright sitting without backrest, front sitting with backrest, front sitting without backrest, left sitting, right sitting	SVM with RBF kernel	97.2%	4 on the seat pan	
(Kamiya, Kudo, Nonaka, & Toyama, 2008)	10	4,500 sets (50 examples*9 postures*10 subjects)	9	Normal, leaning forward, leaning backward, leaning right, right leg crossed, leaning right with right leg crossed, leaning left, left leg crossed, leaning left with left leg crossed	SVM	93%	64 on the seat pan	

In developing a new cushion with sensors that could record characteristics of the occupant behavior, it should be kept in mind that with intensive use pressure sensors at the top of the seat pan could be damaged. To achieve a non-intrusive solution, in other words, reducing the influence on seat comfort, it might be preferable to place the sensors underneath the foam layer, which is distant from the human-seat interface. Theoretically, it could also diminish the noise raised from the wrinkles on the cloth when passengers seated. However, it could be that the patterns are less good recognisable as they are further away from the real human-seat interaction. Therefore, it is important to verify if the pressure patterns can still be recognised in this way. Based on our knowledge, there is no related study on embedding pressure sensors into aircraft seats.

The aim of the study

The purpose of this paper is to study the relationship between different postures and support force sensed by pressure sensors both on the seat pan and under the foam. This study also focuses on whether the pressure distribution underneath the foam layer on the seat is informative enough to recognise common sitting postures of aircraft passengers and how to optimise the position of the pressure sensors to capture sitting posture changes in real time context with a minimum amount of sensors.

The research question is: *Can sensors under the cushion detect sitting postures in an aircraft seat and if so, what is the minimum number of sensors and where should these be located?*

Method

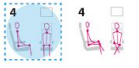


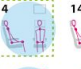




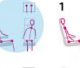

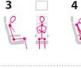
















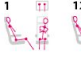








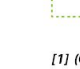





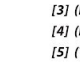
Sitting postures selection (corresponding to activities)


To study the position of the sensors, first postures that people take while traveling are defined based on previous research in aircraft seats. Forty two postures could be found in two papers studying the postures in aircraft seats. From these 42 postures, twelve sitting postures of aircraft passengers are selected, as shown in Table 2. An overview of all common sitting postures in aircraft is presented in Table 3. The research findings from Liu, Yu, and Chu (2019) and Tan, Chen, kimman, & Rauterberg, (2010) are used as a basis. The Liu study (2019) involved 18 subjects sitting in an aircraft cabin for 2h. They were recorded with a camera. 12 postures observed in sleeping and reading, 11 postures observed in using electrical devices, 12 postures observed in reading, and 11 postures observed in watching. In the Tan study (2010), 15 subjects were observed during a 12h long haul flight and it was focused on sleeping positions, which in total 15 postures were observed. There are mainly two considerations for excluding some from these postures they found. Firstly, postures with legs crossed are excluded as in smaller pitches subjects with larger anthropometric values are not able to do that. Secondly, postures with only small variations of the head or arm position are excluded as these might not be found in the pressure sensor results, which was affirmed in a small pilot study.


Table 2. 12 selected sitting postures of aircraft passengers


<p>P1</p>   <p>Head: free from headrest Trunk: upright Arms: free from armrests, on the thigh Legs: both feet on the floor</p>	<p>P7</p>   <p>Head: against headrest Trunk: turned torso, towards right Arms: right arm on right armrest Legs: both feet on the floor</p>
<p>P2</p>   <p>Head: against headrest Trunk: against backrest Arms: free from armrests, on the thigh Legs: both feet on the floor</p>	<p>P8</p>   <p>Head: free from headrest Trunk: against backrest Arms: hold phone on the thigh Legs: both feet on the floor</p>
<p>P3</p>   <p>Head: against headrest Trunk: against backrest Arms: free from armrests, on the thigh Legs: feet crossed at ankle</p>	<p>P9</p>   <p>Head: free from headrest Trunk: against backrest Arms: hold phone in front of chest Legs: both feet on the floor</p>
<p>P4</p>   <p>Head: against headrest Trunk: against backrest, lean left Arms: left arm on left armrest Legs: both feet on the floor</p>	<p>P10</p>   <p>Head: against headrest Trunk: upper back against backrest Arms: free from armrests, on the thigh Legs: feet crossed at ankle</p>
<p>P5</p>   <p>Head: against headrest Trunk: against backrest, lean left Arms: right arm on right armrest Legs: both feet on the floor</p>	<p>P11</p>   <p>Head: against headrest Trunk: upper back against backrest Arms: free from armrests, on the thigh Legs: both feet on the floor</p>
<p>P6</p>   <p>Head: against headrest Trunk: turned torso, towards left Arms: left arm on left armrest Legs: both feet on the floor</p>	<p>P12</p>   <p>Head: free from headrest Trunk: lean forward Arms: on the table in the front Legs: both feet on the floor</p>

Table 3. All sitting postures mentioned in related studies in the context aircraft seats

	Watching IFE	Resting Sleeping Listening to music	Reading Using small electrical devices
Upright			
Against backrest	 	          	    
Slumped	   	       	     
Lean forward		  	  

 Selected sitting postures for the experiment

 The most observed postures in study [4]

 The top two postures in this activity in study [4]

[1] (Ciaccia & Sznclwar, 2012)
 [2] (Hiemstra-van Mastrigt, 2015)
 [3] (Romli, Aminian, & Hamzah, 2019)
 [4] (Liu, Yu, & Chu, 2019)
 [5] (Tan, Chen, Kimman, & Rauterberg, 2010)

Approach of this study

The general method of this study is illustrated in Figure 3. Pressure recordings will be made at the top, which is common in seat pressure distribution studies. Additionally, recordings under the foam are made. It is assumed that under the foam sensors will not be damaged so easily, but it could be that less information is gathered. Based on the calculation of power analysis, 33 subjects might be enough to find significant differences. These 33 subjects were invited to the experiment. Afterwards, a classification model will be made and trained to optimise the number and position of FSR sensors. This experimental protocol was approved by the ethical committee of TU Delft.

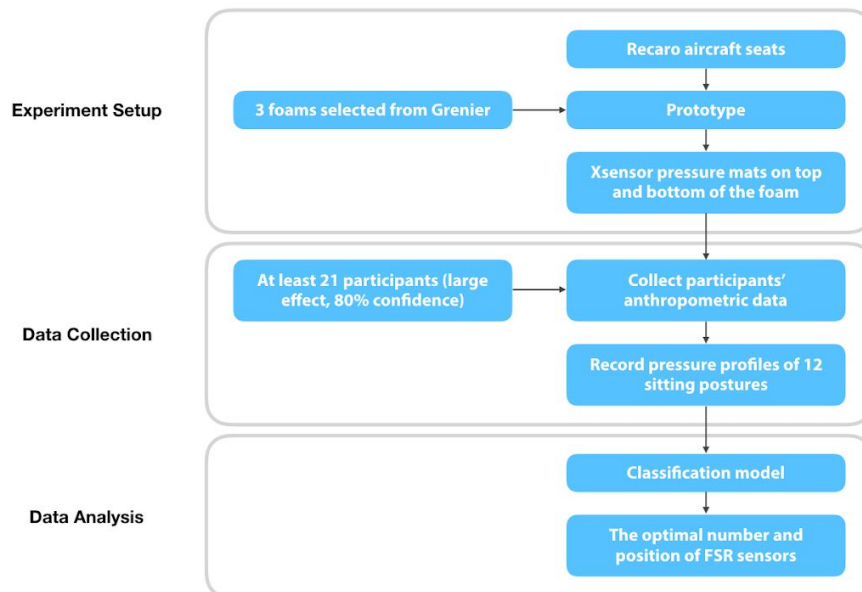


Figure 3. The general approach of this study

Materials & Methods

General descriptions

Pressure profiles were collected of 12 common sitting postures of aircraft passengers on three different types of cushions by using two Xsensor pressure mats, which were placed on the top and bottom of the foam. Each posture was maintained for one minute and the pressure distribution was recorded in 2Hz. This was exported in the CSV format from the software XSENSOR PRO V8 (Xsensor Technology Corporation, 2017). The experiment was set up in the MediaLab SDE in the Faculty of Industrial Design Engineering in TU Delft. 15 female and 18 male ageing from 23 to 37 years old participated in the experiment, with a corresponding BMI ranging from 17.6 to 41.3.

Apparatus

The aircraft seats used for data collection of buttock pressure maps were built on the Recaro BL3520 economy class passenger seat (see Figure 4). In front of the Recaro seats, a row of Zodiac aircraft seats were placed to simulate the 31-inch seat pitch and the tray table behind it was used for the subjects to perform posture 12. Attached to the Recaro seats frame, a seat pan made of medium-density fibreboard (MDF) was created (see Figure 5). The inclination angle of the seat pan was 12 degrees and the angle between seat pan and backrest was 96 degree inspired by the original design of the seats.



Figure 4. The experiment setup

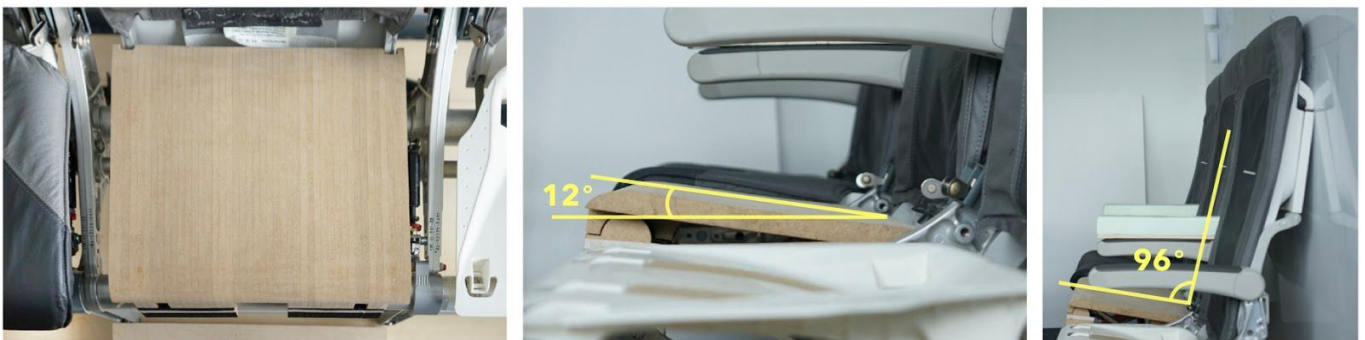



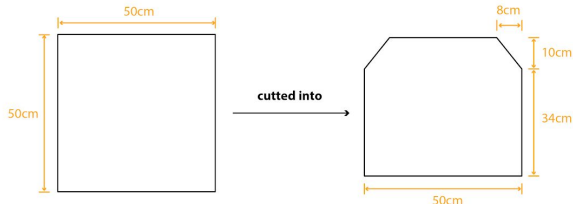
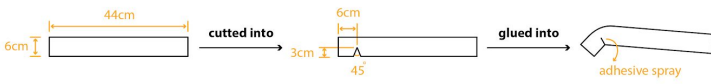


Figure 5. The seat pan made of MDF

Three different foam combinations were provided by Greiner Aerospace, and were made into the shape following the seat pan (see Table 4). Each top layer of the cushion is a 60-mm thick foam, and the bottom layer is 10 mm thick. For cushion B and C, different foam of the top layer were glued by an adhesive spray. The placement of the cushion and the additional 60 mm layer blocks made of polystyrene foam and plywood board are illustrated in Figure 6.

Table 4. The cushion construction method

Top layers of three cushions	  
Top view	
Side view	

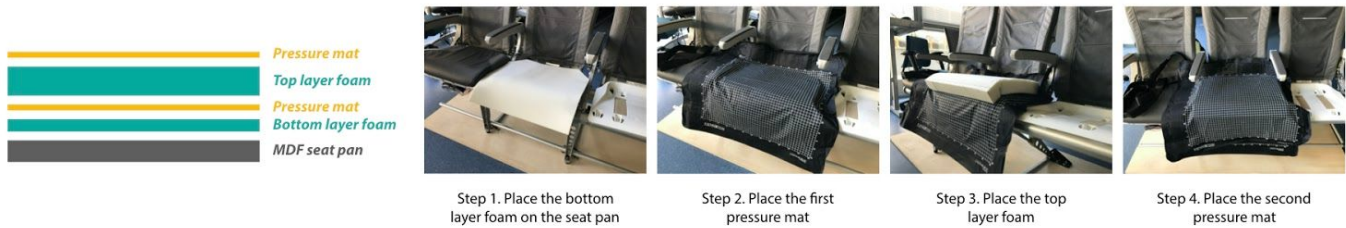


Figure 6. Placement of the foams and pressure mats on the seat pan

The pressure mats, LX210:48.48.02 (see Appendix 1) developed by XSENSOR Technology Corporation were used for measuring buttock pressure distribution. The mat consists of 48 by 48 sensing cells, and the dimension of each cell is 12.7 mm by 12.7 mm. There was no tape used between the different layers of the seat pan structure, but transparent adhesive tape used at the top edges of the pressure mats.

Comfort and discomfort was recorded using a 7-point Likert scale (see Appendix 2) (1 being no comfort and 7 being extreme comfort), (1 being no discomfort and 7 being extreme discomfort). Additionally, local perceived discomfort was recorded (LPD) (1 being no discomfort and 7 being extreme discomfort). The subjects had to rate the score on a body map which was divided into 8 regions according to Hartung (2006). These were measured in a short term (12min) sitting experience for each cushion. The results of the questionnaires were analyzed by Friedman Test, which is a non-parametric statistical test used for comparing three or more matched groups (Riffenburgh, 2012). Therefore, the performance of three cushions on sitting comfort and discomfort can be ranked with statistical significance verified.

Subjects

The demographic and anthropometric characteristics of the subjects are listed in Table 5. The anthropometric measurements followed the definition shown on the DINED database (see Figure 7), including the comparison with the data of the Dutch adult aged from 20 to 30 retrieved from the database (P5, P50, P95) (DINED, 2004) due to 30 subjects were between 20 and 30 and 3 subjects were between 31 to 37.

Table 5. Demographic and anthropometric characteristics of the subjects and the comparison with the data (P5, P50, P95) of the Dutch adults aged from 20 to 30 retrieved from DINED database (2004)

		Min	Average	Max	SD	P5	P50	P95	Left	Right
Male (n = 18)	Age (years)	25.0	26.94	32.0	2.10	-	-	-	-	-
	Stature (cm)	159.5	176.47	196.5	8.62	171.6	184.8	198.0	-	-
	Weight (kg)	47.0	74.94	109.6	16.61	57.0	80.0	103.0	-	-
	BMI (kg / m ²)	17.6	24.13	41.3	5.82	-	-	-	-	-
	Popliteal Height (cm)	39.0	41.92	47.0	2.02	44.6	49.7	54.8	-	-
	Buttock Popliteal Length (cm)	43.0	46.56	51.0	2.78	47.3	52.2	57.1	-	-
	Buttock Knee Length (cm)	55.0	59.72	64.5	3.22	59.7	65.1	70.5	-	-
	Hip Width (cm)	32.5	39.19	49.0	3.80	34.0	38.8	43.6	-	-
	Dominant hand (number of subjects)	-	-	-	-	-	-	-	1	17
Female (n = 15)	Age (years)	23.0	26.60	37.0	3.33	-	-	-	-	-
	Stature (cm)	154.0	164.55	180.6	7.23	157.7	168.7	179.7	-	-
	Weight (kg)	45.6	56.17	72.3	8.10	51.0	66.0	81.0	-	-
	BMI (kg / m ²)	18.0	20.75	26.4	2.75	-	-	-	-	-
	Popliteal Height (cm)	33.5	39.75	43.0	2.33	40.0	44.1	48.2	-	-
	Buttock Popliteal Length (cm)	39.0	44.17	49.5	2.80	45.1	49.7	54.3	-	-
	Buttock Knee Length (cm)	51.2	56.55	63.0	3.91	55.7	61.0	66.3	-	-
	Hip Width (cm)	35.5	37.64	41.5	2.03	35.8	40.2	44.6	-	-
	Dominant hand (number of subjects)	-	-	-	-	-	-	-	2	13
General (n = 33)	Age (years)	23.0	26.79	37.0	2.69	-	-	-	-	-
	Stature (cm)	154.0	171.05	196.5	9.94	158.2	176.1	194.0	-	-
	Weight (kg)	45.6	66.41	109.6	16.29	52.0	73.0	94.0	-	-
	BMI (kg / m ²)	17.6	22.59	41.3	4.93	-	-	-	-	-
	Popliteal Height (cm)	33.5	40.93	47.0	2.39	40.1	46.7	53.3	-	-
	Buttock Popliteal Length (cm)	39.0	45.47	51.0	3.00	45.5	50.8	56.1	-	-
	Buttock Knee Length (cm)	51.2	58.28	64.5	3.85	56.6	62.9	69.2	-	-
	Hip Width (cm)	32.5	38.52	49.0	3.21	34.8	39.6	44.4	-	-
	Dominant hand (number of subjects)	-	-	-	-	-	-	-	3	30

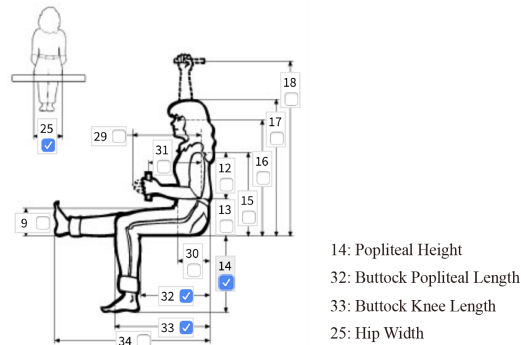


Figure 7. Four anthropometric measurements of the subjects (DINED, 2004)

Experimental protocol

Firstly, the researcher explained the experiment procedure to the subjects, and both signed the informed consent. The demographic data were gathered and the anthropometric data were measured. A manual with 12 sitting postures in a certain sequence with example images and descriptions was given to each subject. The sequence of postures and cushions were systematically varied. After explanation of the postures, the subjects were guided to the first cushion they needed to evaluate. The subjects were instructed to sit in the center of the seat. They adopted the 12 postures one by one under the guidance of the researchers. Each body posture had to be maintained for one minute. The pressure recording lasted for 10s for each posture. After sitting in all the postures, the subject had to leave the seat and completed the questionnaires. At the same time, the second cushion was set up. The procedure followed for the next cushions was the same. The subjects were asked to empty their pockets before the experiment. To exclude bias of visual perception, subjects were kept innocent about the appearance and other information about the cushions.

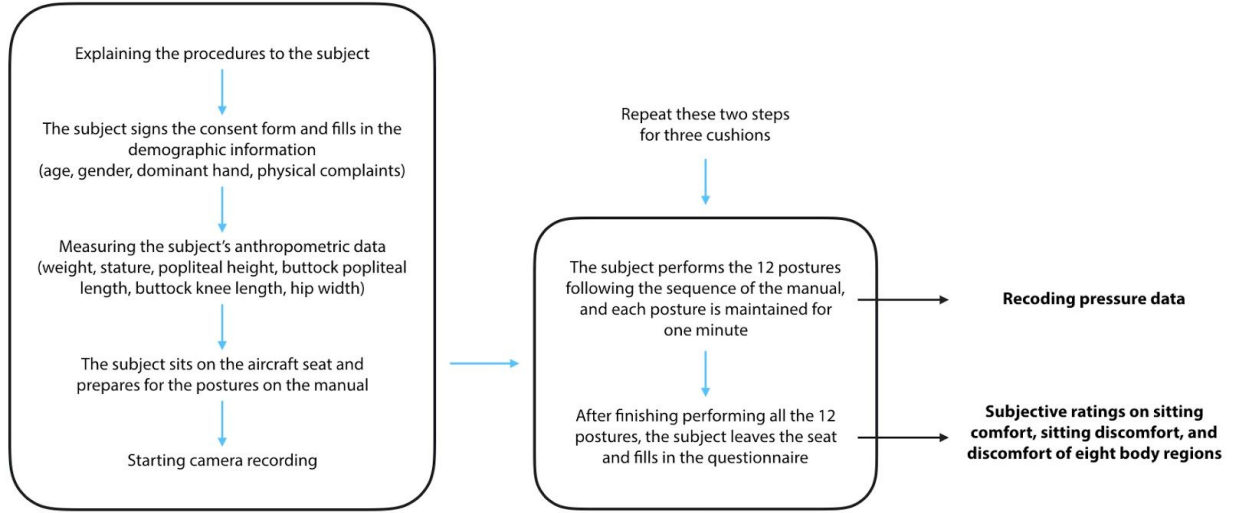


Figure 8. Experimental protocol for each subject

Pressure Data analysis

For each posture, 1980 frames (10s*2Hz*33 subjects*3 cushions) of the top pressure map and the bottom were collected. The mean of the contact areas and pressure at each cell were established. Following the methods developed by Kilincsoy (2019), we divided the contact area into 6 zones and calculated the percentages of the support force of each zone with respect to the total support force.

The pressure mat consists of 48 by 48 cells, each has a size of 12.7mm by 12.7 mm. In the collection of the data, the subjects were instructed to sit in the center of the seat. However, in the real usage scenario, often the passengers do not sit in the center of the seat. To simulate possible deviations for a more robust model, the 48 by 48 cells were shifted around as the example illustrated in Figure 9. In the figure, an element (green) can be moved from left to right (7 grids) and from the backrest toward the front seat (5 grids). Therefore, each set of data was augmented to 35 sets where one is the original dataset, resulting in a total of 24,255 sets of data (bottom only, 35*7 postures*33 subjects*3 cushions). Considering the size of the sensors and the interference between adjacent sensors (Tekscan, n.d.), 4 neighboring cells were grouped together to form a block for measuring the pressure underneath the buttock of the passengers as shown in Figure 10. In the figure, a grid is a cell, and the blue and the green colors indicate the 24 by 24 blocks.

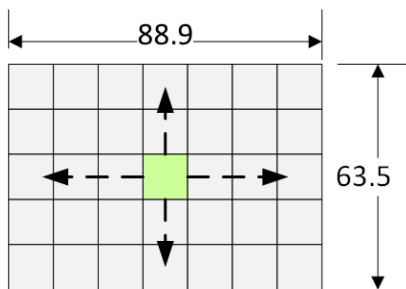


Figure 9. Data argumentation (unit: mm)

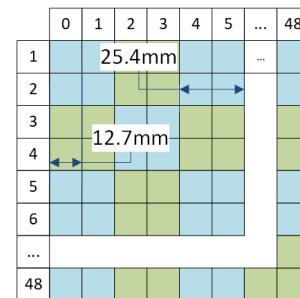


Figure 10. Elements (48 by 48) and blocks (24 by 24) formulated by neighboring elements

Based on the 24,255 sets of 24 by 24 pressure data regarding 12 sitting postures, we first applied the Linear SVC (Support Vector Classifier), SVC with a RBF (radial basis function) kernel, KNN (K-Nearest Neighbor), Random forest and DNN (Deep Neural Network) these five classifiers to find the classifier with the highest classification accuracy. Then we use the SHAP (SHapley Additive exPlanations, Lundberg and Lee (2017)) to explain the classification model and to identify the contributions of each block regarding this model. The block(s) that has the least contribution was iteratively removed until the classification accuracy was less than the threshold (95%). During this process, The remaining blocks were clustered and further discussed regarding the possible number of sensors, the ergonomics setup, the seating postures and the expected classification accuracy. Finally, a set of sensor positions were selected regarding the selected postures that can be predicted with an accuracy of >95%.

Results

Contact area and pressure distribution

In general the results show that for the top layers, the recorded forces are influenced by the contact area while in the bottom layer, the forces are dissipated to a much larger area (see Figure 11). Different postures are linked to different pressure profiles. For instance, in the postures P4, P5, P6, and P7, the concentrated area (“red” regions) of the support is much smaller than other postures. Regarding the different cushions, the contact area of cushion C is smaller than that of the other two types. This is especially true in the bottom layer contact area. It also shows more peak forces as indicated by the larger “red” regions. This could be explained by the fact that the hardness of cushion C is the largest and cushion A is the most soft one.

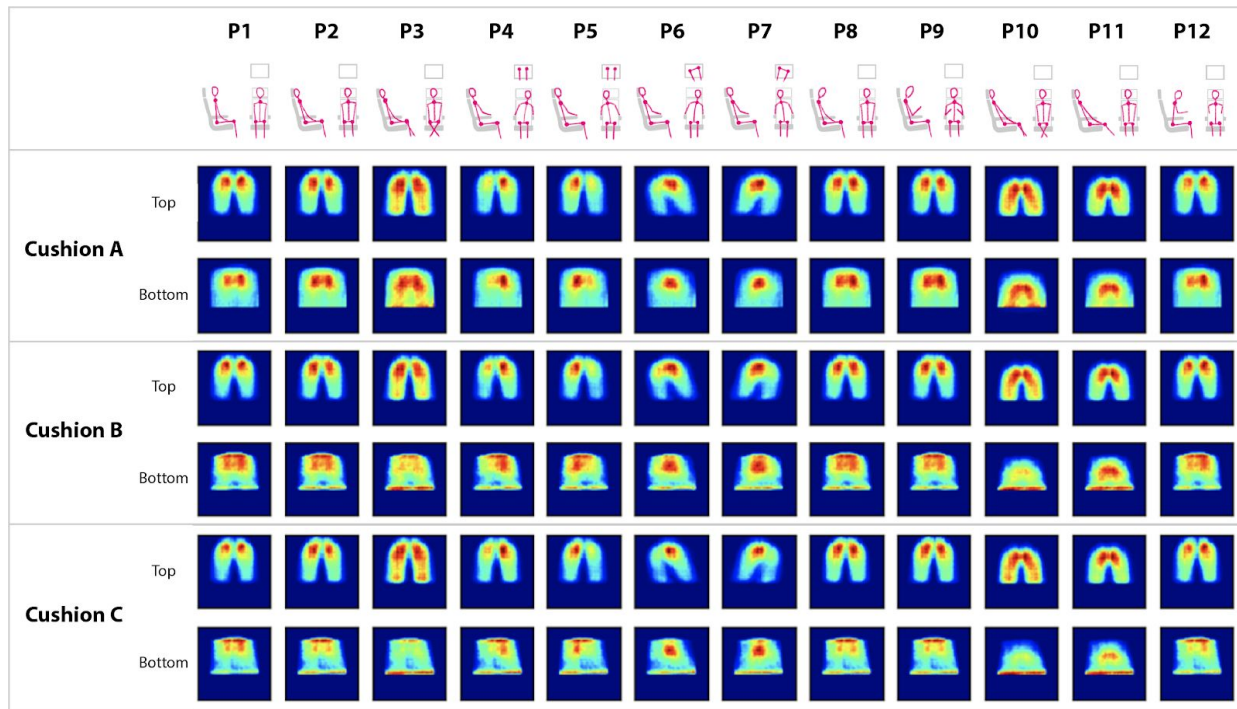


Figure 11. The mean of the top and the bottom pressure in 12 postures regarding 3 types of cushions

Table 6 shows the Pearson correlation between anthropometric parameters and contact area/total pressure. The coefficients highlighted in bold represent that there is a linear correlation between two variables ($p < 0.05$), within which, the higher the coefficient is, the stronger the correlation is. All the correlations shown are positive. Among these seven anthropometric parameters, weight, BMI, buttock knee length, and hip width are strongly correlated with contact area/total pressure regardless of cushion types or pressure maps collected at the top or bottom of the cushion. Increase in weight, BMI, and hip width will result in larger contact area and total pressure. Stature and buttock popliteal length are less strongly correlated with contact area/total pressure. For stature and contact area/total pressure, the correlation only exists at the bottom layer. The increase in stature will result in larger contact area/total pressure. This could be a result of larger weight and BMI of the subject group with higher stature in this study (see Table 7). Too much noise at the top layer could be a reason that the correlation only shows at the bottom layer. For the buttock popliteal length and contact area/total pressure, the correlations exist at top and bottom layers of cushion A and B, but for cushion C this phenomenon was only found at the bottom layer. On the bottom layer, the increase in buttock popliteal length results in larger contact area/total pressure. For popliteal height and contact area/total pressure, there is no correlation found regardless of cushion types or top/bottom layer.

Table 6. Pearson correlation between contact area/total pressure and anthropometric measures (bold letters: $p < 0.05$)

			Weight (kg)	Stature (cm)	BMI (kg/m ²)	Popliteal height (cm)	Buttock popliteal length (cm)	Buttock knee length (cm)	Hip width (cm)
Cushion A	Top	Contact area	0.88	0.21	0.91	0.09	0.35	0.52	0.88
	Top	Total pressure	0.88	0.30	0.86	0.10	0.36	0.46	0.79
	Bottom	Contact area	0.81	0.52	0.66	0.32	0.41	0.57	0.66
	Bottom	Total pressure	0.93	0.45	0.84	0.28	0.46	0.56	0.78
Cushion B	Top	Contact area	0.86	0.16	0.90	0.07	0.37	0.52	0.87
	Top	Total pressure	0.88	0.26	0.88	0.07	0.39	0.47	0.78
	Bottom	Contact area	0.88	0.39	0.80	0.25	0.43	0.57	0.78
	Bottom	Total pressure	0.94	0.42	0.86	0.24	0.48	0.59	0.81
Cushion C	Top	Contact area	0.85	0.12	0.92	0.04	0.33	0.50	0.88
	Top	Total pressure	0.86	0.22	0.88	0.05	0.34	0.44	0.80
	Bottom	Contact area	0.87	0.39	0.80	0.26	0.43	0.61	0.79
	Bottom	Total pressure	0.94	0.40	0.88	0.23	0.46	0.60	0.84

Table 7. Mean (SD) of weight, BMI, and hip width of lower and higher group of the subjects

	Number of subjects	Weight (kg)	BMI (kg/m ²)	Hip width (cm)
Stature < 1761 mm	20	66.41 (16.61)	22.59 (4.93)	38.52 (3.21)
Stature ≥ 1761 mm	13	76.88 (12.36)	23.5 (3.66)	39.31 (2.59)

Figure 12 shows the correlations between weight, BMI, and hip width with contact area, respectively. In general, cushion A has the largest contact area and the increasing rate of it is larger on the top layer than on the bottom layer. On the top layer, the contact area on cushion A is the largest, followed by cushion B, and on cushion C is the smallest given the same weight, BMI, or hip width. The rate of increase of contact area on these three cushions is similar. On the bottom layer, although the contact area on cushion A is the largest, while on cushion B and C, the contact areas are very close to each other, which indicates a similar mechanical behavior of cushion B and C. The increasing rate of contact area on cushion A is slightly smaller than it is on cushion B and C.

Table 8 shows the Friedman test results of the questionnaire. The mean ranks highlighted in bold represent that the rankings of 3 different cushions are significant ($p < 0.05$). It shows that cushion A had the highest comfort score and cushion C had the lowest. For the buttock areas and upper thigh areas, cushion C had the highest discomfort score and cushion A had the lowest. For the right lumbar area, cushion C had the highest discomfort score and cushion B had the lowest.

By dividing the subjects into two groups based on BMI (10 subjects' larger than 24.9), it shows that the high BMI group experienced more discomfort in buttock areas. When dividing the subjects into two groups based on average stature of Dutch adults aged from 20 to 30 (13 subjects' higher than 1761mm), it shows that the high-stature group experienced more discomfort in lumbar and buttock areas.

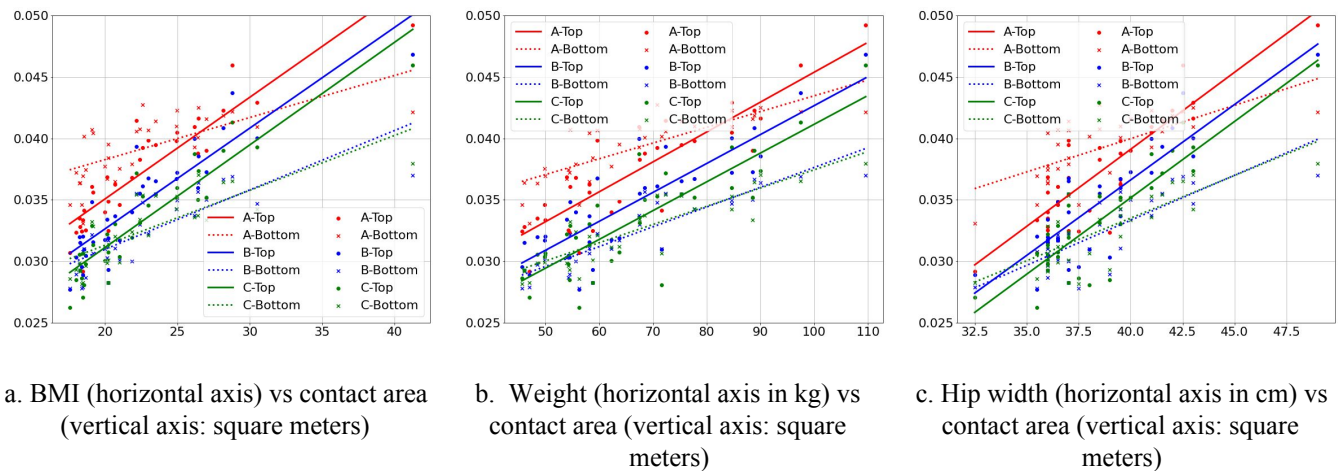
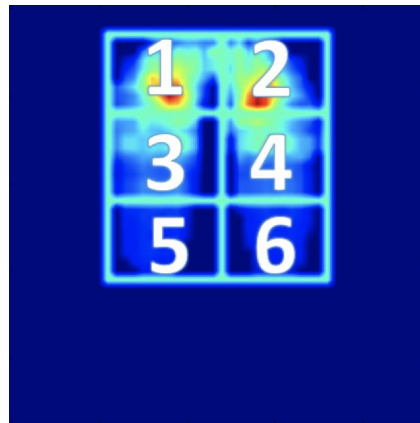


Figure 12. BMI, Weight and Hip width vs contact areas

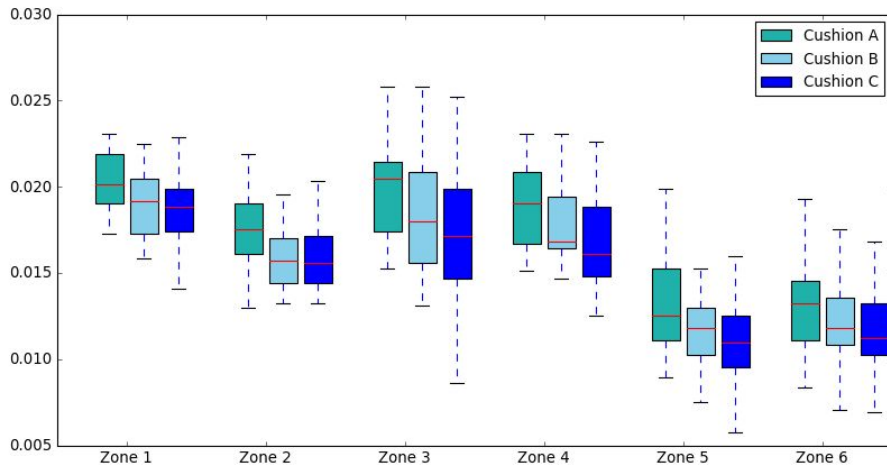
Table 8. Friedman test results of questionnaire

		Mean Rank			p - value
		Cushion A	Cushion B	Cushion C	Asymp. Sig.
All subjects (n = 33)	General sitting comfort	2.27	2.08	1.65	0.020
	General sitting discomfort	1.83	1.91	2.26	0.117
	LPD - left lumbar	2.08	1.73	2.20	0.051
	LPD - right lumbar	2.06	1.71	2.23	0.031
	LPD - left buttock	1.65	2.02	2.33	0.006
	LPD - right buttock	1.59	2.06	2.35	0.002
	LPD - left upper thigh	1.74	2.00	2.26	0.028
	LPD - right upper thigh	1.74	2.00	2.26	0.028
	LPD - left lower thigh	1.85	2.03	2.12	0.321
	LPD - right lower thigh	1.82	2.08	2.11	0.247
		Mean Rank			p - value
		Cushion A	Cushion B	Cushion C	Asymp. Sig.
BMI < 25 (n = 23)	General sitting comfort	2.20	2.15	1.65	0.076
	General sitting discomfort	1.96	1.85	2.20	0.394
	LPD - left lumbar	2.11	1.70	2.20	0.077
	LPD - right lumbar	2.07	1.72	2.22	0.106
	LPD - left buttock	1.76	1.96	2.28	0.119
	LPD - right buttock	1.70	2.00	2.30	0.061
	LPD - left upper thigh	1.78	1.98	2.24	0.138
	LPD - right upper thigh	1.80	1.93	2.26	0.124
	LPD - left lower thigh	1.85	2.09	2.07	0.510
	LPD - right lower thigh	1.83	2.13	2.04	0.408
		Mean Rank			p - value
		Cushion A	Cushion B	Cushion C	Asymp. Sig.
BMI ≥ 25 (n = 10)	General sitting comfort	2.45	1.90	1.65	0.164
	General sitting discomfort	1.55	2.05	2.40	0.102
	LPD - left lumbar	2.00	1.80	2.20	0.565
	LPD - right lumbar	2.05	1.70	2.25	0.289
	LPD - left buttock	1.40	2.15	2.45	0.023
	LPD - right buttock	1.35	2.20	2.45	0.016
	LPD - left upper thigh	1.65	2.05	2.30	0.179
	LPD - right upper thigh	1.60	2.15	2.25	0.141
	LPD - left lower thigh	1.85	1.90	2.25	0.368
	LPD - right lower thigh	1.80	1.95	2.25	0.350
		Mean Rank			p - value
		Cushion A	Cushion B	Cushion C	Asymp. Sig.
Stature < 1761 mm (n = 20)	General sitting comfort	2.25	2.10	1.65	0.091
	General sitting discomfort	1.78	1.93	2.30	0.161
	LPD - left lumbar	2.08	1.63	2.30	0.032
	LPD - right lumbar	2.03	1.65	2.33	0.043
	LPD - left buttock	1.68	1.93	2.40	0.030
	LPD - right buttock	1.65	1.98	2.38	0.028
	LPD - left upper thigh	1.75	2.00	2.25	0.141
	LPD - right upper thigh	1.78	1.95	2.28	0.133
	LPD - left lower thigh	1.85	2.15	2.00	0.465
	LPD - right lower thigh	1.83	2.20	1.98	0.320
		Mean Rank			p - value
		Cushion A	Cushion B	Cushion C	Asymp. Sig.
Stature ≥ 1761 mm (n = 13)	General sitting comfort	2.31	2.04	1.65	0.212
	General sitting discomfort	1.92	1.88	2.19	0.622
	LPD - left lumbar	2.08	1.88	2.04	0.804
	LPD - right lumbar	2.12	1.81	2.08	0.519
	LPD - left buttock	1.62	2.15	2.23	0.135
	LPD - right buttock	1.50	2.19	2.31	0.050
	LPD - left upper thigh	1.73	2.00	2.27	0.195
	LPD - right upper thigh	1.69	2.08	2.23	0.177
	LPD - left lower thigh	1.85	1.85	2.31	0.169
	LPD - right lower thigh	1.81	1.88	2.31	0.174

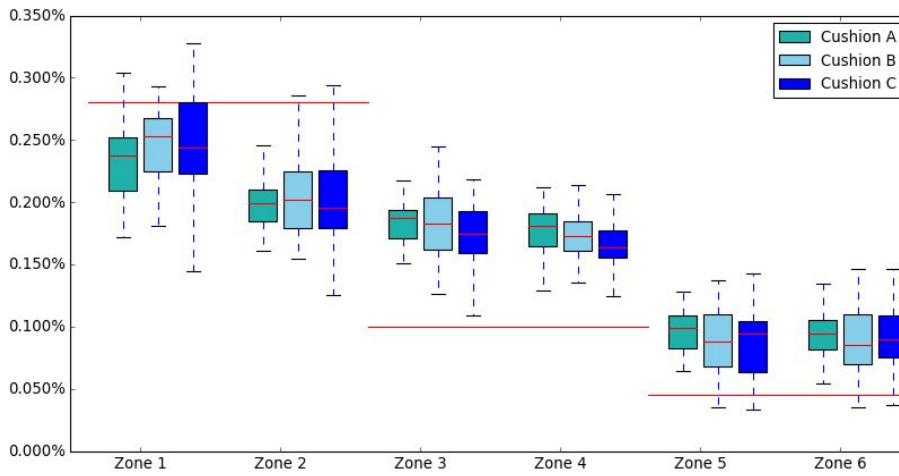
Figure 13 shows the most comfortable pressure distribution following the principle of Kilincsoy (2019). In Figure 13(a), an example is presented to indicate the 6 zones that were used in the analysis. In Figure 13(b), the contact area of each zone is presented in a box plot. In the figure cushion C has the smallest contact areas for all zones and cushion A has the largest. The distribution of forces between Zone 5 and 6, and between Zone 3 and 4 are similar. However, zone 1 and 2 are statistically significantly different ($p < 0.01$). Compared to the ideal distribution for comfort found in Kilincsoy (see Figure 13(c)), the distributions have quite large differences regarding all three types of cushions.



(a) An example of the 6 zones



(b) Contact areas of each zone (vertical axis unit: m²)



(c) The percentage of the support force in each zone regarding the sum of the support force, red lines indicate the ideal percentage of support force in each zone of an SUV back seat (Zone 1,2: 29.5%, Zone 3,4: 20%, Zone 5,6: 6%) (vertical axis unit: the percentage of the total pressure)

Figure 13. Analysis of the support force of the upright posture (Posture 2) following Kilincsoy's method

Investigation of positions and numbers of FSR sensors at the bottom of the cushion

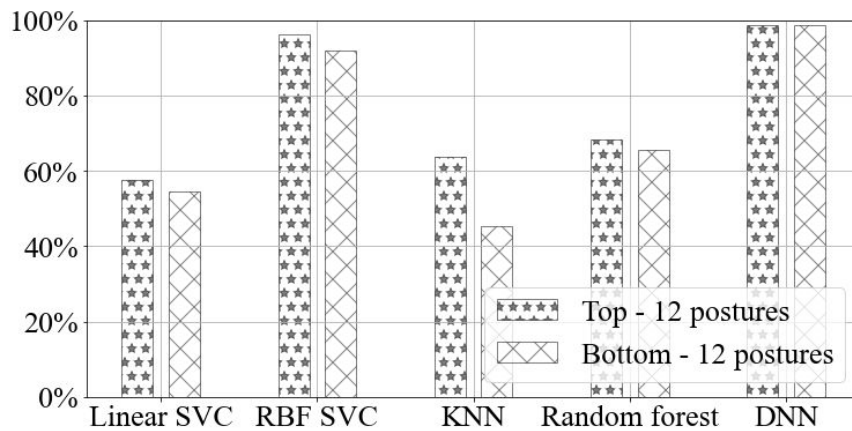


Figure 14. Classification of postures using different classifier

Figure 14 presents the 12-posture classification results using different classifiers based on the top and the bottom measurements, respectively. In the figure, it can be found that using the DNN performs the best in the classification, the next are the RBF based SVC, the KNN and the random forest classifiers. The accuracy is the lowest when the linear SVC method was used, most probably due to the nonlinear relations between the postures and the collected pressure data. It is worth mentioning that in the classification, where the data of all cushions were combined, the performance of the DNN was still able to reach nearly 100% (99.44% for using the top pressure data and 99.48% for using the bottom pressure data). The consistent high performances of the DNN classifier across different types of cushions offer the opportunities of developing one solution for these three types of cushions.

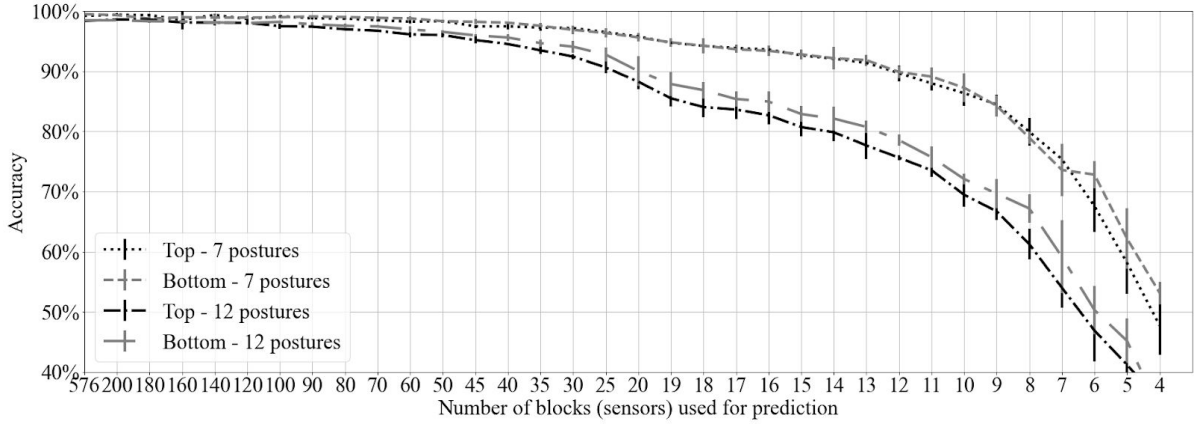


Figure 15: The performance of the DNN classifier regarding the used number of blocks

Using the DNN classifier and the SHAP values, we iteratively remove blocks with the least contribution. Figure 15 presents that accuracy of the classification in this iterative process. It was found that when the amount of sensors was reduced, the classification accuracy of 12 postures was decreased. The accuracy of the classifier is lower than 90% when the number of used blocks is less than 20. To further reduce the number of blocks while maintaining a high level of accuracy, among the 12 postures, 7 are selected for building a new classification model.

The reason for choosing these 7 postures (P2, P4, P5, P6, P7, P11, and P12) was that there was not much variance observed from the mean pressure maps of excluded postures and selected postures (see Figure 11), which in detail were 1) excluding P1: the trunk-thigh angle of P1 is slightly smaller than P2 due to the small backrest angle of the Recaro seat, therefore, the mean pressure maps of P1 and P2 are similar. Besides, P2 is a much more common posture performed for long duration instead of P1 by aircraft passengers; 2) excluding P3: P3 is with legs crossed at the ankle while P2 is without legs crossed. Although the mean pressure maps of P2 and P3 show great difference in front area of the seat, the difference mainly exists in the group with a small popliteal height. Because of enabling feet on the floor, more pressure of lower thigh area was distributed for those group of subjects; 3) excluding P10: excluding is because of a similar reason as the previous one when comparing it with P11; 4) excluding P8: P8 is with head down when looking at the phone held on the thigh, while P2 is with head against the headrest. This variation was not transformed clearly to the pressure maps under the buttock; 5) excluding P9: P9 is with the head looking down at the phone held when arms are against armrests. Again, no clear variation with P2.

The variations were even more not obvious on the bottom layer. Using these 7 selected postures, it can be found that the accuracy of the classification can be higher than 90% when more than 12 sensors are used. Another interesting discovery is that the using the data collected from the bottom pressure mat had nearly the same, and some time even better classification accuracy than using the data collected from the top pressure mat. This is especially true when the number of blocks were reduced.

Figure 16 presents the relations with the mean pressure of P2. 26 blocks that contribute most to the classification based on the SHAP values and the final selected 15 blocks for predicting the 7 postures. It can be found that those blocks are mainly located in the area around buttock and thigh. Cross-validation (10-fold) indicated that the proposed DNN model was able to reach an 99.0% accuracy in identifying those 7 postures using data collected from the aforementioned 15 positions. Figure 17 presents the contribution (SHAP value) of sensors in the aforementioned 15 positions to the final classification. SHAP (SHapley Additive exPlanations) proposed by Lundberg and Lee (2017) explains how much each predictor contributes to the prediction, which bridges the interpretability to accuracy. In this case, it can be found that: 1) all blocks contribute to the classification of 7 postures and 2) data collected from block 2, 3, 4, 5, 6 contribute the most to the classification.

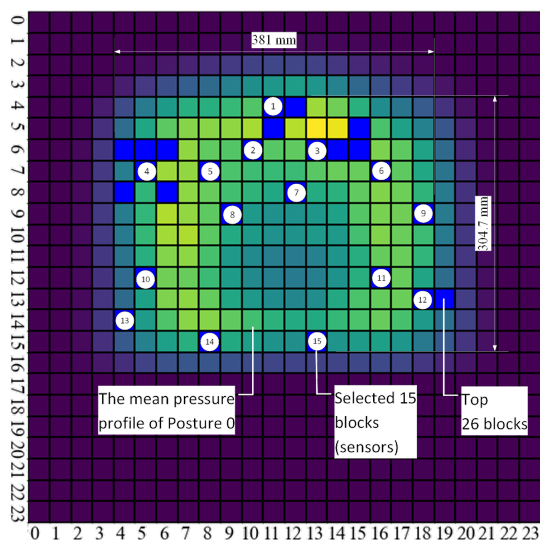


Figure 16. Selection of sensor positions

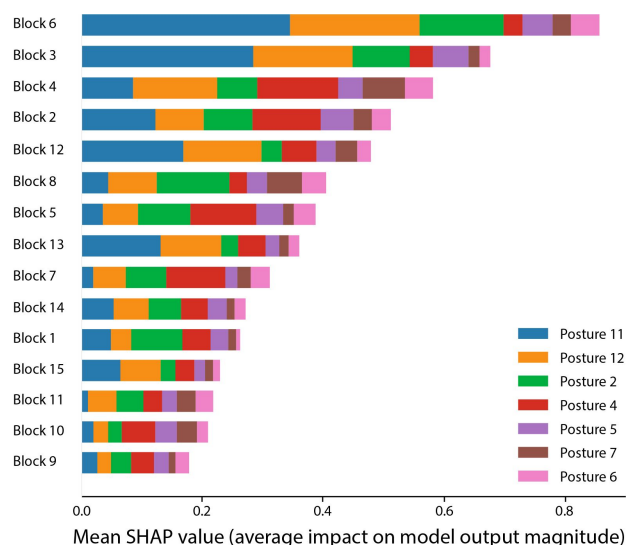


Figure 17. SHAP values of the 15 sensor positions to predict 7 sitting postures

Discussion

The results in this study showed that sitting postures can be detected by placing multiple FSR pressure sensors underneath the foam on the seat pan, even more accurately than placing them on the top of the foam. This can be explained by the fact that the pressure data collected at the bottom is more robust regardless of foam materials, noise of cloth and wrinkles. By focusing on the possibility of recognising postures from the bottom of the cushion, the passengers' sitting behavior can be objectively monitored in real time by a non-intrusive manner, which would minimise the influence of subjective feelings of comfort. Additionally, it could reduce the cost and computational power compared with using a pressure mat or pressure sensor matrix. The durability of the sensors can be extended when embedding them at the bottom instead of at the top of the cushion as well.

In the experiment, the pressure data were collected based on a flat seat pan made by MDF, which is not the real case in aircraft seats. Moreover, it was measured statically in a laboratory environment, however, the actual flying conditions would also influence the pressure distribution. Therefore, a study is recommended to embed the 15 sensors into commercial aircraft cushion and test it in the real context. To further recognise in-seat movements such as postural changes and fidgeting, it requires more pressure variables as input such as center of pressure and the percentage and duration of weight shifts ((Leban, Aripa, Fancello, Fadda, & Pau, 2019; Sonenblum & Sprigle, 2018).

Ergonomics

We selected 15 out of 256 sensor positions that contribute most to the prediction of 7 postures. In the previous studies, the sensor positions were mostly placed asymmetrically (Halabi, Fawal, Almughani, and Al-Homsi, 2017; Mutlu, Krause, Forlizzi, Guestrin, & Hodgins, 2007; Meyer, Arnrich, Schumm, & Tröster, 2010), although Liang, Cao, and Liu (2017) selected 10 sensors symmetrically on a 5*8 sensor grid. These studies selected the positions based on certain algorithms and did not mention the percentage of left or right-handed people in their subject groups. Subjects with different dominant hands do produce different pressure distributions under buttock (see Figure 18). The right-handed people generally distribute more load on the left-side of the cushion observed from the pressure maps, and more load distributed on the right-side of the cushion by left-handed people. Therefore, the asymmetric sensor distribution might be a result of an unbalanced selection of the subject groups in terms of dominant hand. In our study, 30 out of 33 subjects were right-handed, which reflected the percentage of the real-world, therefore we mixed the data as one set. For a better understanding of the difference between the sitting pressure distributions of left- and the right-hand subjects, further investigation with more left-hand subjects is needed.

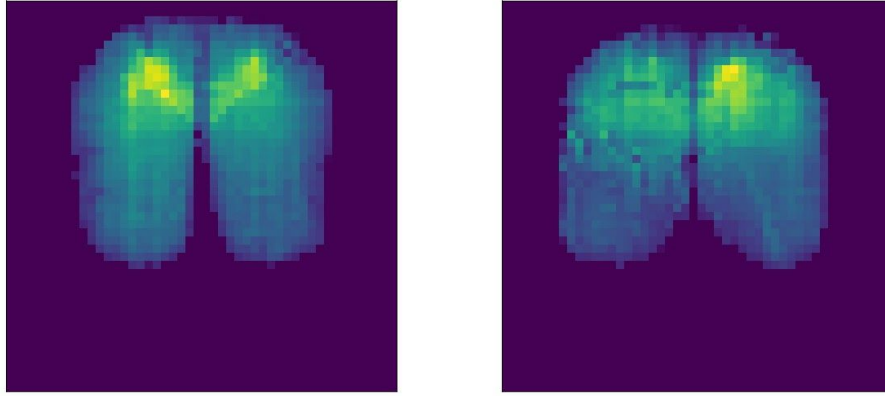


Figure 18. Pressure distributions of P1 by a left-hand (left) and a right-hand (right) subjects

In addition to the influence on pressure distribution of the dominant hand, the sensor positions selected in this study need to be verified in practice since in airline travelling. Though in the data augmentation we tried to simulate different seating positions of the passengers, people that sit next to strangers might tend to shift their body towards the side without any passengers (e.g. windows and aisles). However, if people fly with family or friends, the situation would be different.

Data augmentation & the selection of classifiers

Quality of data:

Researchers revealed that BMI is correlated with the contact area between the buttock and the cushion, which is in accordance with this study. In this study, it was paid special attention to the specificity of data by selecting the subjects for the divergence in BMI. The range of weight and stature of the subjects both covered P5 to P95 measurements of Dutch adults aged from 20 to 30. In accordance with the studies of Ma, Li, Gravina, and Fortino (2017) (4 underweight, 4 normal weight, 4 overweight, ranging from 16 to 34) and Fragkiadakis, Dalakleidi, and Nikita (2019) (2 underweight, 7 normal weight, 3 overweight), the subjects' BMI in our study covered three categories ranging from 17.6 to 41.3 including 4 underweight, 19 normal weight, and 10 overweight. It has been proved that pressure distribution pattern are significantly different among three BMI groups that would further influence the sitting discomfort (Khamis, Tee, Tahir, & Sabri, 2019; Horváth, Antal, Domljan, & Dénes, 2017; Jin, Cheng, Wang, Tao, & Shen, 2011). Ma and his colleagues (2017) compared the classification results of with and without BMI as a feature for prediction. It showed that their sensor placement solution was fit for different body size groups without user-dependent information as an input. Therefore, to recognise sitting postures for a broader population, the selection of subjects should be representative regarding different body size groups.

Data augmentation:

In the data augmentation, we did not mirror the data to augment left-handed people as only 3 out of 33 subjects are left-handed. The limited number of subjects did not provide enough evidence that the right-handed behavior can be mirrored to left-handed people. As 90% of people are right-handed, it is clear that the left-handed people are influenced by the right-handed world.

The pressure maps collected were augmented following the practical usage scenario. In the experiment, the subject was instructed to sit in the center of the cushion, however, the middle line of the pressure maps were not always aligned with the middle line of the pressure mats due to cognitive differences. In addition, the position of the pressure mats could be slightly moved when the subject changed their postures. Therefore, for each pressure map, it was shifted from left to right (7 grids) and back to front (5 grids) based on the observation from raw pressure data collected from both pressure mats.

Data amount and classifier comparisons:

In our study, the pressure data on bottom layer was argument into 24,255 sets (35×7 postures \times 33 subjects \times 3 cushions) to apply the classifiers. The amount of the data sets is comparable and larger than the most of the related works (see Table 1). Various classifiers have been explored in our and previous studies. In our case, DNN outperformed Linear SVC, RBF based SVC, KNN, Random Forest in terms of posture recognition accuracy based on the aforementioned amount of data .

Classification results

In addition to evaluating the performance of different classifiers, we also compared the accuracy of recognising 12 and 7 postures from top and bottom layer respectively. When recognizing 12 postures, the accuracy would be decreased while the

amount of sensors were reduced. The accuracy of the classification is lower than 90% when the number of used blocks is less than 20. When recognizing 7 postures, the accuracy of the classification can be higher than 90% when more than 12 sensors are used.

It was found that using the pressure data collected from the bottom pressure mat has nearly the same accuracy as from the top layer. Sometimes it even achieved even more accuracy. Our assumption here is that the foam layer reduces the noise from cloth and wrinkles, therefore, the pressure projected on the bottom layer can represent a more accurate pressure distribution pattern of the subject.

Calculating the SHAP values of the 256 positions helped us to iteratively remove those block(s) with the least contribution. As a result, 15 out of 256 positions were selected for sensor placement. As presented in Table 1, in the study of Mutlu, Krause, Forlizzi, Guestrin, and Hodgins (2007), 19 sensors were placed both on the surface of the backrest and seat pan to recognise 10 postures with an accuracy of 78%. Zemp and his colleagues (2016) used 16 sensors placed on the armrests, backrest and seat pan to recognise 7 postures with an accuracy of 90.9%. They also explored only using sensors on the seat pan, and the accuracy decreased to 81.9%. In our study, we used the similar amount of sensors placed only on the seat pan and underneath the foam layer, which successfully recognised 7 postures with a relatively high accuracy of 99.0%.

In terms of positions of limited sensors on the seat pan, most of the studies distribute them in a uniform manner. Only a few explored the solutions of placement of sensors in different positions for the best performance of the classification. In accordance with the results from the studies of Mutlu, Krause, Forlizzi, Guestrin, and Hodgins (2007), Zemp et al. (2016), and Liang, Cao, and Liu (2017), it can be observed that the sensors mostly placed in two areas on the seat pan, one is close to the front edge, and the other is at the back under the buttock area.

In terms of contribution of each sensor to the prediction, this study identified 15 sensors were mainly underneath the buttock area. This discovery is different from the outcomes of Zemp et al. (2016), where the most important sensor positions were mainly located in the front of the cushion (calculated by the Random Forest Feature Importance method). Similarly, in the study of Meyer, Arnrich, Schumm, and Tröster (2010), the 14 most important sensor positions selected by the SFS algorithm were also mainly in the front. A possible explanation is that in our study, the sensors were located underneath the foam instead of on the top of it. The changes of pressure distribution of the lower thigh area is more obvious when placing the sensors on the top of the foam. However, due to the different amplitudes of the forces between the thigh and the buttock (Kilincsoy, 2019), such changes are less obvious in the data collected from the bottom pressure mat. Meanwhile, due to the filtering effects introduced by the foams, data collected from the buttock area is more accurate.

Pressure distribution

The results of this experiment showed a different pressure distribution with the Kilincsoy study (2019). In our study, the area that gives the most support force is shifted towards the thigh. This might be the result of a different trunk-thigh angle between seat pan and backrest. In Kilincsoy's study on pressure distribution, subjects could adjust the angle between seat pan and backrest while it was mentioned in another study that the most comfortable trunk-thigh angle for upright position for car passengers is 105(5.5) degree (mean(SD)) degree (Kilincsoy, Wagner, Bengler, Bubb, & Vink, 2014). However, in this study, the seat used is Recaro BL3520 and the angle between backrest and seat pan was fixed to 96 degree in (Figure 5), which may result in a smaller trunk-thigh angle at the same postures. This small trunk-thigh angle may indicate a posture with the weight of the upper body moving towards the knee. The shifting of the largest support force area reflects the change of center of gravity.

Conclusion

This study explored the possibility of recognizing sitting postures by using FSR pressure sensors at the bottom layer of the cushion on the seat pan. With the pressure profiles of 12 sitting postures collected from both top and bottom layer of 3 cushions, multiple classifiers were applied and the DNN classifier had the best performance. For recognising 7 out of 12 postures, with an accuracy of 99.0%, a 15-sensor placement solution at the bottom layer was proposed based on the DNN classifier and SHAP value. It demonstrated the possibility of embedding FSR pressure sensors at the bottom of the cushion to recognise sitting behavior. The results of this study could provide opportunities in further study of detecting sitting comfort and discomfort in a non-intrusive manner, as well as new IoT solutions for a better cabin service towards comfort of passengers.

Acknowledgement

The authors want to express their appreciation to Greiner Aerospace for providing cushion materials. We also want to appreciate the ethical committee in TU Delft for their support in the ethical clearance regarding COVID-19 measures. Lastly but most importantly, we want to thank all the subjects of the experiment, especially regarding taking all measures in this COVID-19 pandemic period.

References

- Ahram, T. Z., & Falcão, C. S. (2018). Smart Blanket: A Real-Time User Posture Sensing Approach for Ergonomic Designs Bo. *Advances in Intelligent Systems and Computing*, 607, 1–15. <https://doi.org/10.1007/978-3-319-60492-3>
- Ai, H., Zhang, L., Yuan, Z., & Huang, H. (2018). ICushion: A Pressure Map Algorithm for High Accuracy Human Identification. *Proceedings - International Conference on Pattern Recognition*, 2018-August, 3483–3488. <https://doi.org/10.1109/ICPR.2018.8545671>
- Anjani, S., Li, W., Ruiter, I. A., & Vink, P. (2020). The effect of aircraft seat pitch on comfort. *Applied Ergonomics*, 88(June), 103132. <https://doi.org/10.1016/j.apergo.2020.103132>
- Bang, Y. H., Kang, D. W., Choi, J. S., Mun, K. R., Tack, G. R., & Jang, K. B. (2010). Body pressure measuring device for the prevention against pressure sores. *I-CREAtE 2010 - International Convention on Rehabilitation Engineering and Assistive Technology*.
- Campos, G. H., & Xi, F. J. (2020). Pressure sensing of an aircraft passenger seat with lumbar control. *Applied Ergonomics*, 84(October 2017), 103006. <https://doi.org/10.1016/j.apergo.2019.103006>
- Ciaccia, F. R. D. A. S., & Sznclwar, L. I. (2012). An approach to aircraft seat comfort using interface pressure mapping. *Work*, 41(SUPPL.1), 240–245. <https://doi.org/10.3233/WOR-2012-0163-240>
- DARMA (2019). Darma Smart Cushion. Retrieved from: <https://www.gadgenda.com/darma-smart-cushion>
- DINED (2004). Anthropometric database, Delft University of Technology. Retrieved from: <https://dined.io.tudelft.nl/en/about>
- Fasulo, L., Naddeo, A., & Cappetti, N. (2019). A study of classroom seat (dis)comfort: Relationships between body movements, center of pressure on the seat, and lower limbs' sensations. *Applied Ergonomics*, 74(August 2018), 233–240. <https://doi.org/10.1016/j.apergo.2018.08.021>
- Fragkiadakis, E., Dalakleidi, K. V., & Nikita, K. S. (2019). Design and Development of a Sitting Posture Recognition System. *Proceedings of the Annual International Conference of the IEEE Engineering in Medicine and Biology Society, EMBS*, 3364–3367. <https://doi.org/10.1109/EMBC.2019.8856635>
- Gavish, I., & Brenner, B. (2011). Air travel and the risk of thromboembolism. *Internal and Emergency Medicine*, 6(2), 113–116. <https://doi.org/10.1007/s11739-010-0474-6>
- Gravina, R., & Li, Q. (2019). Emotion-relevant activity recognition based on smart cushion using multi-sensor fusion. *Information Fusion*, 48(August), 1–10. <https://doi.org/10.1016/j.inffus.2018.08.001>
- Halabi, O., Fawal, S., Almughani, E., & Al-Homsi, L. (2017). Driver activity recognition in virtual reality driving simulation. *2017 8th International Conference on Information and Communication Systems, ICICS 2017*, 111–115. <https://doi.org/10.1109/IIACS.2017.7921955>
- Hartung, J. (2006). Objektivierung des statischen Sitzkomforts auf Fahrzeugsitzen durch die Kontaktkräfte zwischen Mensch und Sitz. Retrieved from: <https://d-nb.info/980169062/34>

- Helander, M. G., & Zhang, L. (1997). Field studies of comfort and discomfort in sitting. *Ergonomics*, 40(9), 895–915.
<https://doi.org/10.1080/001401397187739>
- Hiemstra-Van Mastrigt, S. (2015). Comfortable passenger seats: Recommendations for design and research (PhD Thesis). Retrieved from: <https://doi.org/10.4233/uuid:eedd25e6-c625-45e9-9d32-f818aa89c19d>
- Hiemstra-van Mastrigt, S., Groenesteijn, L., Vink, P., & Kuijt-Evers, L. F. M. (2017). Predicting passenger seat comfort and discomfort on the basis of human, context and seat characteristics: a literature review. *Ergonomics*, 60(7), 889–911.
<https://doi.org/10.1080/00140139.2016.1233356>
- Hiemstra-Van Mastrigt, S., Meyenborg, I., & Hoogenhout, M. (2016). The influence of activities and duration on comfort and discomfort development in time of aircraft passengers. *Work*, 54(4), 955–961. <https://doi.org/10.3233/WOR-162349>
- Hiemstra-Van Mastrigt, S., Smulders, M., Bouwens, J. M. A., & Vink, P. (2019, August 30). Designing aircraft seats to fit the human body contour. *DHM and Posturography*, 2019, 781-789.
<http://dx.doi.org/10.1016/B978-0-12-816713-7.00061-1>
- Horváth, P. G., Antal, R. M., Domljan, D., & Dénes, L. (2017). Body pressure distribution maps used for sitting comfort visualization. *Sigurnost*, 59(2), 123–132.
- Huang, Y. R., & Ouyang, X. F. (2012). Sitting posture detection and recognition using force sensor. 2012 5th International Conference on Biomedical Engineering and Informatics, BMEI 2012, Bmei, 1117–1121.
<https://doi.org/10.1109/BMEI.2012.6513203>
- IATA (2018) IATA Forecast Predicts 8.2 billion Air Travelers in 2037. Retrieved from:
<https://www.iata.org/en/pressroom/pr/2018-10-24-02/>
- Ishac, K., & Suzuki, K. (2018). Lifechair: A conductive fabric sensor-based smart cushion for actively shaping sitting posture. *Sensors (Switzerland)*, 18(7). <https://doi.org/10.3390/s18072261>
- Jin, X., Cheng, B., Wang, B., Tao, X., & Shen, B. (2011). Evaluation and prediction of driver comfort using body pressure sensors. *Proceedings - 3rd International Conference on Measuring Technology and Mechatronics Automation, ICMTMA 2011*, 2, 72–75. <https://doi.org/10.1109/ICMTMA.2011.305>
- Kamiya, K., Kudo, M., Nonaka, H., & Toyama, J. (2008). Sitting posture analysis by pressure sensors. *Proceedings - International Conference on Pattern Recognition*, December. <https://doi.org/10.1109/icpr.2008.4761863>
- Khamis, N. K., Tee, N. C., Tahir, M. F. M., & Sabri, N. (2019). Pattern of pressure distribution on the car seat under static condition and its relationship with driving posture. *International Journal of Innovative Technology and Exploring Engineering*, 8(12), 4189–4194. <https://doi.org/10.35940/ijitee.L3668.1081219>
- Kilincsoy, Ü. (2019). Digitalization of posture-based seat design (PhD Thesis). The ideal pressure distribution for SUV and sedan rear seats. Retrieved from: <https://doi.org/10.4233/uuid:419e4678-cb27-4c03-9725-7fb5b0fd3a12>
- Kilincsoy, Ü., Wagner, A., Bengler, K., Bubbs, H., & Vink, P. (2014). Comfortable rear seat postures preferred by car passengers. *5th International Conference on Applied Human Factors and Ergonomics*, 20(January), 30–40.
- Kilincsoy, Ü., Wagner, A., Vink, P., & Bubbs, H. (2016). Application of ideal pressure distribution in development process of automobile seats. *Work*, 54(4), 895–904. <https://doi.org/10.3233/WOR-162350>
- Kim, D. G., Wang, C., Ho, J. G., Min, S. D., Kim, Y., & Choi, M. H. (2020). Development and feasibility test of a capacitive belt sensor for noninvasive respiration monitoring in different postures. *Smart Health*, 16(January), 100106.
<https://doi.org/10.1016/j.smhl.2020.100106>
- Kim, M., Kim, H., Park, J., Jee, K. K., Lim, J. A., & Park, M. C. (2018). Real-time sitting posture correction system based on highly durable and washable electronic textile pressure sensors. *Sensors and Actuators, A: Physical*, 269, 394–400.
<https://doi.org/10.1016/j.sna.2017.11.054>

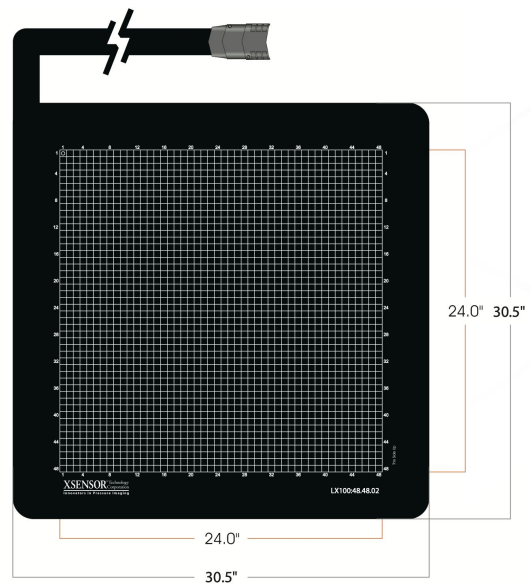
- Kim, Y. M., Son, Y., Kim, W., Jin, B., & Yun, M. H. (2018). Classification of children's sitting postures using machine learning algorithms. *Applied Sciences (Switzerland)*, 8(8). <https://doi.org/10.3390/app8081280>
- Le, P., Rose, J., Knapik, G., & Marras, W. S. (2014). Objective classification of vehicle seat discomfort. In *Ergonomics* (Vol. 57, Issue 4, pp. 536–544). Taylor & Francis. <https://doi.org/10.1080/00140139.2014.887787>
- Leban, B., Arippa, F., Fancello, G., Fadda, P., & Pau, M. (2019). Analysis of Discomfort During a 4-Hour Shift in Quay Crane Operators Objectively Assessed Through In-Chair Movements: Vol. VI (Issue January). Springer International Publishing. <https://doi.org/10.1007/978-3-319-96074-6>
- Li, W., Yu, S., Yang, H., Pei, H., & Zhao, C. (2017). Effects of long-duration sitting with limited space on discomfort, body flexibility, and surface pressure. *International Journal of Industrial Ergonomics*, 58, 12–24. <https://doi.org/10.1016/j.ergon.2017.01.002>
- Liang, G., Cao, J., & Liu, X. (2017). Smart cushion: A practical system for fine-grained sitting posture recognition. 2017 IEEE International Conference on Pervasive Computing and Communications Workshops, PerCom Workshops 2017, 7, 419–424. <https://doi.org/10.1109/PERCOMW.2017.7917599>
- Liu, J., Yu, S., & Chu, J. (2019). The Passengers' Comfort Improvement by Sitting Activity and Posture Analysis in Civil Aircraft Cabin. *Mathematical Problems in Engineering*, 2019. <https://doi.org/10.1155/2019/3278215>
- Liu, W., Guo, Y., Yang, J., Hu, Y., & Wei, D. (2019). Sitting posture recognition based on human body pressure and CNN. *AIP Conference Proceedings*, 2073(February). <https://doi.org/10.1063/1.5090747>
- Low, E., Sam, T. H., Tee, K. S., Rahim, R. A., Saim, H., Zakaria, W. N. W., Khialdin, S. M., Isa, H., & Soon, C. F. (2020). Development of a wireless and ambulatory posture monitoring system. *International Journal of Integrated Engineering*, 12(2), 170–176. <https://doi.org/10.30880/ijie.2020.12.02.020>
- Lundberg, S., & Lee, S. (2017). A Unified Approach to Interpreting Model Predictions. 31st Conference on Neural Information Processing Systems. NIPS 2017.
- Ma, C., Li, W., Gravina, R., Cao, J., Li, Q., & Fortino, G. (2017). Activity level assessment using a smart cushion for people with a sedentary lifestyle. *Sensors (Switzerland)*, 17(10), 1–19. <https://doi.org/10.3390/s17102269>
- Ma, S., Cho, W. H., Quan, C. H., & Lee, S. (2016). A sitting posture recognition system based on 3 axis accelerometer. *CIBCB 2016 - Annual IEEE International Conference on Computational Intelligence in Bioinformatics and Computational Biology*, 1–3. <https://doi.org/10.1109/CIBCB.2016.7758131>
- Martins, L., Ribeiro, B., Pereira, H., Almeida, R., Costa, J., Quaresma, C., Jesus, A., & Vieira, P. (2015). Real-Time Fuzzy Monitoring of Sitting Posture: Development of a New Prototype and a New Posture Classification Algorithm to Detect Postural Transitions. *BIOSTEC 2015. Communications in Computer and Information Science*, vol 574. Springer, Cham. https://doi.org/10.1007/978-3-319-27707-3_26
- Mergl, C. (2006). Entwicklung eines Verfahrens zur Optimierung des Sitzkomforts auf Automobilsitzen [Development of a Method for Optimizing the Seating Comfort of Automotive Seats] (Doctoral dissertation). 156. <http://nbn-resolving.de/urn/resolver.pl?urn:nbn:de:bvb:91-diss20060518-1108310685>
- Meyer, J., Arnrich, B., Schumm, J., & Troster, G. (2010). Design and modeling of a textile pressure sensor for sitting posture classification. *IEEE Sensors Journal*, 10(8), 1391–1398. <https://doi.org/10.1109/JSEN.2009.2037330>
- Mutlu, B., Krause, A., Forlizzi, J., Guestrin, C., & Hodgins, J. (2007). Robust, low-cost, non-intrusive sensing and recognition of seated postures. *UIST: Proceedings of the Annual ACM Symposium on User Interface Software and Technology*, January, 149–158. <https://doi.org/10.1145/1294211.1294237>
- Naddeo, A., Califano, R., & Vink, P. (2018). The effect of posture, pressure and load distribution on (dis)comfort perceived by students seated on school chairs. *International Journal on Interactive Design and Manufacturing*, 12(4), 1179–1188. <https://doi.org/10.1007/s12008-018-0479-3>

- Qian, Z., Bowden, A. E., Zhang, D., Wan, J., Liu, W., Li, X., Baradoy, D., & Fullwood, D. T. (2018). Inverse piezoresistive nanocomposite sensors for identifying human sitting posture. *Sensors (Switzerland)*, 18(6), 1–16. <https://doi.org/10.3390/s18061745>
- Riffenburgh, R. H. (2012). Tests on Ranked Data. *Statistics in Medicine*, 221–248. <https://doi.org/10.1016/b978-0-12-384864-2.00011-1>
- Roh, J., Park, H. J., Lee, K. J., Hyeong, J., Kim, S., & Lee, B. (2018). Sitting posture monitoring system based on a low-cost load cell using machine learning. *Sensors (Switzerland)*, 18(1), 1–18. <https://doi.org/10.3390/s18010208>
- Romano, E., Pirozzi, M., Ferri, M., Calcante, A., Oberti, R., Vitale, E., & Rapisarda, V. (2019). The use of pressure mapping to assess the comfort of agricultural machinery seats. *International Journal of Industrial Ergonomics*, February 2018, 102835. <https://doi.org/10.1016/j.ergon.2019.102835>
- Romli, F. I., Aminian, N. O., & Hamzah, N. A. (2019). Identification of common sitting postures of aircraft passengers through observation method. *International Journal of Recent Technology and Engineering*, 7(6), 218–221.
- Sammonds, G. M., Fray, M., & Mansfield, N. J. (2017). Effect of long term driving on driver discomfort and its relationship with seat fidgets and movements (SFMs). *Applied Ergonomics*, 58, 119–127. <https://doi.org/10.1016/j.apergo.2016.05.009>
- SENSIMAT (2014). Retrieved from: <https://www.sensimatssystems.com/>
- Smulders, M., Berghman, K., Koenraads, M., Kane, J. A., Krishna, K., Carter, T. K., & Schultheis, U. (2016). Comfort and pressure distribution in a human contour shaped aircraft seat (developed with 3D scans of the human body). *Work*, 54(4), 925–940. <https://doi.org/10.3233/WOR-162363>
- Sonenblum, S. E., & Sprigle, S. H. (2018). Some people move it, move it... for pressure injury prevention. *Journal of Spinal Cord Medicine*, 41(1), 106–110. <https://doi.org/10.1080/10790268.2016.1245806>
- Tan, C. F., Chen, W., Kimman, F., & Rauterberg, M. (2010). Sleeping in sitting posture analysis of economy class aircraft passenger. *Lecture Notes in Electrical Engineering*, 60 LNEE(May 2014), 703–713. https://doi.org/10.1007/978-90-481-8776-8_60
- Tatsuno, J., & Maeda, S. (2019). Development of Simple Detection Method of Involuntary Movements to Evaluate Human Discomfort in Vehicle Seat. *Advances in Intelligent Systems and Computing*, 786, 857–865. https://doi.org/10.1007/978-3-319-93885-1_80
- Tekscan (n.d.). FlexiForce Integration Guides. Retrieved from: <https://www.tekscan.com/flexiforce-integration-guides>
- Vink, P., & Hallbeck, S. (2012). Editorial: Comfort and discomfort studies demonstrate the need for a new model. *Applied Ergonomics*, 43(2), 271–276. <https://doi.org/10.1016/j.apergo.2011.06.001>
- Vink, P., Overbeeke, C. J., & Desmet, P. M. A. (2004). Comfort experience. *Comfort and Design: Principles and Good Practice*, 1–12. <https://doi.org/10.1201/9781420038132.ch1>
- Wegner, M.B. (2020). Seat comfort objectification (PhD Thesis). Retrieved from: <https://doi.org/10.4233/uuid:b772802d-b738-4312-8903-9eedfab62e6e>
- Xsensor Technology Corporation (2017). XSENSOR PRO V8: New PRO software for pressure testing and measurement.
- Xsensor Technology Corporation (2017). Testing and Measurement Product Catalogue. Retrieved from: <https://www.nbn-elektronik.ch/shop/files/XSensor-Uebersicht-der-Druckmesssysteme-zur-Druckverteilungsanalyse.pdf>
- Xu, W., Li, Z., Huang, M. C., Amini, N., & Sarrafzadeh, M. (2011). eCushion: An eTextile device for sitting posture monitoring. *Proceedings - 2011 International Conference on Body Sensor Networks, BSN 2011*, 1(c), 194–199. <https://doi.org/10.1109/BSN.2011.24>

- Zemp, R., Tanadini, M., Plüss, S., Schnüriger, K., Singh, N. B., Taylor, W. R., & Lorenzetti, S. (2016). Application of Machine Learning Approaches for Classifying Sitting Posture Based on Force and Acceleration Sensors. *BioMed Research International*, 2016. <https://doi.org/10.1155/2016/5978489>
- Zemp, R., Taylor, W. R., & Lorenzetti, S. (2015). Are pressure measurements effective in the assessment of office chair comfort/discomfort? A review. *Applied Ergonomics*, 48, 273–282. <https://doi.org/10.1016/j.apergo.2014.12.010>
- Zenk, R., Franz, M., Bubb, H., & Vink, P. (2012). Technical note: Spine loading in automotive seating. *Applied Ergonomics*, 43(2), 290–295. <https://doi.org/10.1016/j.apergo.2011.06.004>
- Zhang, L., Helander, M. G., & Drury, C. G. (1996). Identifying factors of comfort and discomfort in sitting. *Human Factors*, 38(3), 377–389. <https://doi.org/10.1518/001872096778701962>
- Zhang, Y., Huang, Y., Lu, B., Ma, Y., Qiu, J., Zhao, Y., Guo, X., Liu, C., Liu, P., & Zhang, Y. (2020). Real-time sitting behavior tracking and analysis for rectification of sitting habits by strain sensor-based flexible data bands. *Measurement Science and Technology*, 31(5). <https://doi.org/10.1088/1361-6501/ab63ea>
- Zhao, C., Yu, S. huai, Harris Adamson, C., Ali, S., Li, W. hua, & Li, Q. qian. (2020). Effects of aircraft seat pitch on interface pressure and passenger discomfort. *International Journal of Industrial Ergonomics*, 76(October 2018), 102900. <https://doi.org/10.1016/j.ergon.2019.102900>
- Zhao, C., Yu, S. huai, Miller, C., Ghulam, M., Li, W. hua, & Wang, L. (2019). Predicting aircraft seat comfort using an artificial neural network. *Human Factors and Ergonomics In Manufacturing*, 29(2), 154–162. <https://doi.org/10.1002/hfm.20767>
- Zhu, Y., Qiu, S., Li, M., Chen, G., Hu, X., Liu, C., & Qu, X. (2019). A Smart Portable Mat That Can Measure Sitting Plantar Pressure Distribution with a High Resolution. 2019 IEEE 6th International Conference on Industrial Engineering and Applications, ICIEA 2019, 141–144. <https://doi.org/10.1109/IEA.2019.8714871>

Appendices

Appendix 1. Xsensor pressure mat LX210:48.48.02 (Xsensor Technology Corporation, 2017)



Appendix 2. Questionnaire of general sitting comfort, general sitting discomfort and local perceived discomfort

General sitting comfort questionnaire (from 1 to 7): ○ ○ ○ ○ ○ ○ ○

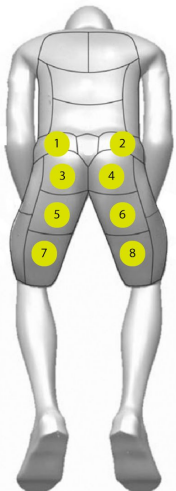
○ ○ ○ ○ ○ ○ ○
No comfort Extreme comfort

General sitting discomfort questionnaire (from 1 to 7): ○ ○ ○ ○ ○ ○ ○

○ ○ ○ ○ ○ ○ ○
No discomfort Extreme discomfort

LPD Questionnaire (from 1 to 7):

○ ○ ○ ○ ○ ○ ○
No discomfort Extreme discomfort



1 (Left lumbar)	2 (Right lumbar)
○ ○ ○ ○ ○ ○ ○	○ ○ ○ ○ ○ ○ ○
3 (Left buttock)	4 (Right buttock)
○ ○ ○ ○ ○ ○ ○	○ ○ ○ ○ ○ ○ ○
5 (Left upper thigh)	6 (Right upper thigh)
○ ○ ○ ○ ○ ○ ○	○ ○ ○ ○ ○ ○ ○
7 (Left lower thigh)	8 (Right lower thigh)
○ ○ ○ ○ ○ ○ ○	○ ○ ○ ○ ○ ○ ○

Appendix 3. Body mass and stature distribution of 33 subjects and the population of dutch adult aged from 20 to 30 (DINED, 2004)

It shows the distribution of all the 33 subjects represented by the green circles on the map of body mass and stature. The blue dots and the ellipse represent the population of Dutch adults aged from 20 to 30 (DINED, 2004).

